Quantitative Evaluation of Alveolar Bone Resorption on Dental Panoramic Radiographs by Standardized Dentition Image Transformation and Probability Estimation*

Chisako Muramtsu, Ryo Takahashi, Tatsuro Hayashi, Takeshi Hara, Tatsumasa Fukui, Akitoshi Katsumata, and Hiroshi Fujita, *Member, IEEE*

Abstract— **Alveolar bone resorption, which can be observed on dental panoramic radiographs (DPRs), is one of the most important signs of the progression of periodontal disease. However, quantitative and consistent evaluation of alveolar bone resorption is labor intense, because of a large number of DPR examinations performed each year. In our previous study, we developed an automated scheme for detection of three lines, corresponding to an occlusion line, an alveolar line and a root apex line, to measure the alveolar bone ratio (ABR), which may be useful to dentists in early detection of periodontal disease. In this study, we propose a new image transformation that maps the tooth region to a standardized dentition image for improved visualization and detection of alveolar crest points by probability estimation. The proposed method was applied to 92 DPRs with 4 degrees of alveolar bone resorption. The ABR measurement obtained by the proposed method was compared with the manual measurement of alveolar bone loss (ABL). In this preliminary investigation, the computer-estimated ABR was moderately correlated with the manual ABL. The result indicates the potential usefulness of the method for early detection and consistent diagnosis of periodontal disease.**

I. Introduction

Periodontal disease is a common dental disease which affects many adults. The presence of alveolar bone resorption is one of the important signs of periodontal disease. In general, the degree of bone resorption is assessed by probing in which a blunted needle-like instrument is inserted to a gap between tooth and gum for the depth measurement. The examination can cause pain and bleeding, and the measurement is subjected to intra and inter-operator variabilities. An alternative choice may be the assessment of the level of alveolar bone using x-ray imaging.

Conventionally, the evaluation of alveolar bone loss (ABL) [1] on x-ray images is performed with intraoral radiography. However, it takes time and effort to image and evaluate all of the teeth with intraoral radiographs. On the other hand, a total tooth condition in general dental examination is often evaluated using a dental panoramic radiograph (DPR). Although the spatial resolution is not as good as the intraoral radiographs, DPR is suitable in observing the whole dental region and for evaluating the overall ABL.

A quantitative assessment method for ABL on DPRs is not yet established, and the manual measurement of all the teeth is labor intense. In our previous study [2], we proposed an automated method for detecting three lines corresponding to the levels of tooth occlusions, alveolar crests and root apices. Using the three lines, an alveolar bone ratio (ABR), which can be a surrogate to ABL, was determined. However, detection of these lines was difficult and the performance was not sufficient. The purpose of this study is to investigate a semi-automatic method for quantitative assessment of alveolar bone resorption on DPRs. In this study, we propose a new image transformation by straightening a row of teeth to create a standardized dentition image for better visualization of bone resorption and for automatic detection of alveolar crests based on the Hessian matrix and probability estimation.

II. Database

DPR database used in this study consists of 92 cases obtained with QR master-P™ (Telesystems Co., Ltd., Osaka, Japan) at the Asahi University Dental Hospital. The matrix size is 1573 x 3039 pixels with approximately 0.1 mm per pixel resolution. All images were reviewed by a dental radiologist and graded into 4 degrees of alveolar bone resorption levels. The number of cases assessed as normal, mild, moderate, and severe are 39, 38, 11, and 4, respectively. In addition, ABL was measured at 3 locations each on the right and left lower jaw by a dentist.

III. Methods

A. Overview of the Proposed Method

A flowchart of the proposed method is shown in Fig. 1. First, a standardized dentition image was created by transforming a curved dental region to the straightened row of teeth. Locally dark spots were detected on the basis of the eigenvalues of the Hessian matrix. The feature points corresponding to the alveolar crest were selected by the maximum posterior (MAP) estimation [3]. Measurements of ABR were made using the selected points. An alveolar crest line was determined by spline interpolation for visual assistance.

*Research supported in part by a Grants-in-Aid for Scientific Research (B) (No. 26293402) by Japan Society for the Promotion of Science and a Grants-in-Aid for Scientific Research on Innovative Areas (Multidisciplinary Computational Anatomy, No. 26108005) by Ministry of Education, Culture, Sports, Science and Technology, Japan.

C. Muramatsu, T. Hara, and H. Fujita are with the Department of Intelligent Image Information, Graduate School of Medicine, Gifu University, Gifu, 501-1194 Japan (phone: +81-58-230-6518; fax: +81-58-230-6514; e-mail: chisa@ fjt.info.gifu-u.ac.jp).

R. Takahashi was with the Department of Intelligent Image Information, Graduate School of Medicine, Gifu University, Gifu, 501-1194 Japan. He is now with Densan System Co. Ltd., Gifu, 501-6196 Japan.

T. Hayashi is with Media Co., Ltd., Tokyo, 113-0033 Japan.

T. Fukui and A. Katsumata are with the Department of Oral Radiology, Asahi University School of Dentistry, Mizuho, 501-0296 Japan.

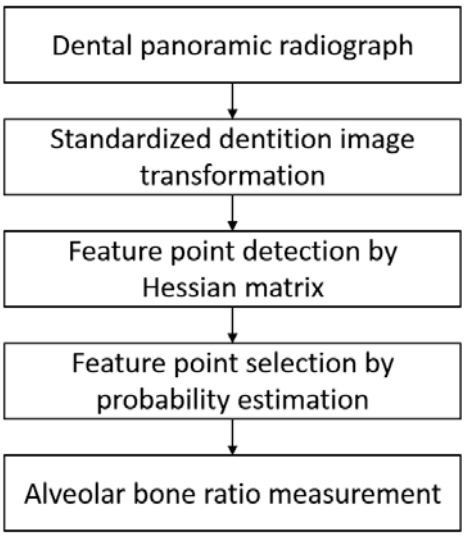

Figure 1. Flowchart of the proposed scheme

B. Standardized Dentition Image Transformation

ABL is determined by the fraction of the decrease in alveolar crest level from the cementoenamel junction. However, the cementoenamel junction is not easily visualized on DPRs. Therefore, our target is to measure an ABR, which is the ratio of the distance between the alveolar crest and the root apex to the height of the tooth.

In our previous automated method [2], features points corresponding to the top of tooth crowns, alveolar crests, and root apices were detected, and the second degree polynomial curve was fitted to each set of points. In this study, a curved region including the teeth was straightened to a rectangular region showing the aligned row of teeth, which we called a standardized dentition image, as shown in Fig. 2. Using the transformed image, detection of alveolar crest points can be facilitated. Such an image can also be helpful to dentists to visually inspect the resorption state.

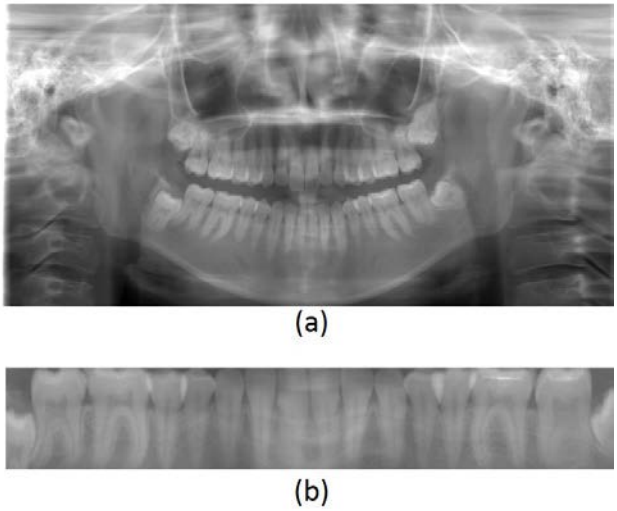

Figure 2. Image transformation. (a) Original dental panoramic radiograph and (b) standardized dentition image

For the image transformation, tooth crown and root apex feature points must be identified. In this study, these points were manually identified. For single rooted teeth, one point was identified whereas for double rooted teeth, two points were identified. Correspondingly, for molar teeth, two points were marked at the cusp. For missing teeth, points were interpolated using the neighbor tooth points. Four end points were extrapolated using the fitted polynomial curves.

For a pair of crown and apex points, 10 equally spaced points were placed for preventing distortion in the standardized dentition image. Using these points as the control points, the tooth region was transformed using a thin plate spline method [4].

C. Detection of Alveolar Crest Points

The points of alveolar crests are observed as dark triangular spots between teeth on DPRs. For detecting these interdental apertures, the Gaussian smoothing was first applied, and the second derivative was computed to obtain the Hessian matrix. Based on the first and second eigenvalues, cup regions, i.e., dark spots, were detected as the candidates of alveolar crest points.

In standardized dentition images, each tooth is approximately aligned. Therefore, the location of the alveolar crest between specific teeth can be limited. Using a mask with 15 sub-regions, only one point in each region was selected from the candidates.

The selection was based on the MAP estimation using following equations.

$$\vec{x}_{MAP} = \underset{\vec{x}}{\operatorname{argmax}} f(\vec{v}|\vec{x}) g(\vec{x}) \tag{1}$$

$$f(\vec{v}|\vec{x}) = p_I(I) p_G(G) p_\theta(\theta) p_S(\lambda_1, \lambda_2) \tag{2}$$

$$g(\vec{x}) = \frac{1}{2\pi} \exp\{-\frac{1}{2}(\vec{x}-\mu)^T \Sigma (\vec{x}-\mu)\} \tag{3}$$

$$p_I(I) = 1 - \frac{\bar{I}}{\max(I)} \tag{4}$$

$$p_G(G) = \frac{\bar{G}}{\max(G)} \tag{5}$$

$$p_\theta(\theta) = \begin{cases} 1 - \dfrac{|\theta - \theta_c|}{\pi/2} & (\theta - \theta_c < \dfrac{\pi}{2}) \\ 0 & (otherwise) \end{cases} \tag{6}$$

$$p_S(\lambda_1, \lambda_2) = -\frac{4}{\pi} \tan^{-1}\left(\frac{\lambda_1 + \lambda_2}{\lambda_1 - \lambda_2}\right) + 2 \tag{7}$$

The likelihood function, $f(\vec{v}|\vec{x})$, is based on the probabilities of image features, *I, G, θ,* λ_1, and λ_2, which correspond to the pixel value, gradient strength, gradient direction with respect to the standard direction, θ_c, and the first and second eigenvalues of the Hessian matrix, respectively. The prior probability, $g(\vec{x})$, is determined by the average, μ, and covariance matrix, Σ, of the coordinates of the gold standard alveolar crest points provided by the dentist.

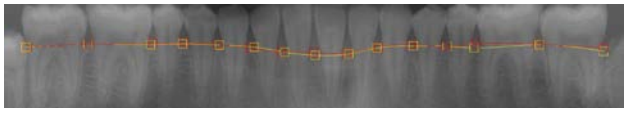

Figure 3. Comparison of alveolar crest points and lines representing the alveolar bone level. (red:detection result, yellow: the gold standard by dentist)

D. ABR Measurement and Evaluation

With the selected points, ABRs were measured and averaged for a case. For perceptive assistance, the points were connected using a spline interpolation. The average ABR measurement results were compared with the average manual ABLs. For evaluation, a leave-one-out cross validation method was used in determination of the prior probability for the MAP estimation.

IV. RESULT

Fig. 3 shows the detected alveolar crest points and the line representing the alveolar bone level. It also shows the points manually determined by the dentist. For this case, the results agree well. The relationship between the average manual ABL provided by the dentist and the average ABR determined by the proposed method is shown in Fig. 4. The correlation coefficient was -0.51. One of the reasons for misdetection of crest points was that the dark spots corresponding to the interdental apertures were large due to missing teeth and not identified as cup regions by the Hessian analysis. Another possible reason for misselection of candidate crest points was that the true crest regions were located in low prior probability regions because the database includes only small numbers of moderate and severe cases.

Figs. 5 and 6 show the average ABLs and ABRs, respectively, for cases with different alveolar bone resorption grades. The ABLs show an increasing trend with the increasing severity of the alveolar bone resorption. Similarity, the ABRs determined by the proposed method show a decreasing trend with the severity. Both grades and ABLs were subjectively assessed by the dentist at different sessions. However, it can be observed that they are not in perfect agreement, indicating the difficulty of such assessments.

Fig. 7 shows the receiver operating characteristic (ROC) curves for distinguishing between normal and other three groups by ABL and ABR. The area under the curve (AUC) for using ABL was 0.81, whereas that using ABR was 0.70. The results indicate the potential usefulness of the proposed method for detection of patients with periodontal disease. However, the AUCs are not very high, even with the manual ABL. These results are partly due to the fact that the database includes a small number of severe cases and the majorities of them are normal and mild. Detection of mild cases is very difficult.

The proposed standardized dentition image transformation can be helpful in facilitating the visual assessment by dentists. Moreover, this format, which is similar to a dental formula for recording dental condition of each tooth, can be used for computerized dental reporting combined with automated detection of dental cavities and fillings. Such a system may support an efficient reporting. The current problem in transformation is the distortion near missing teeth and tilted

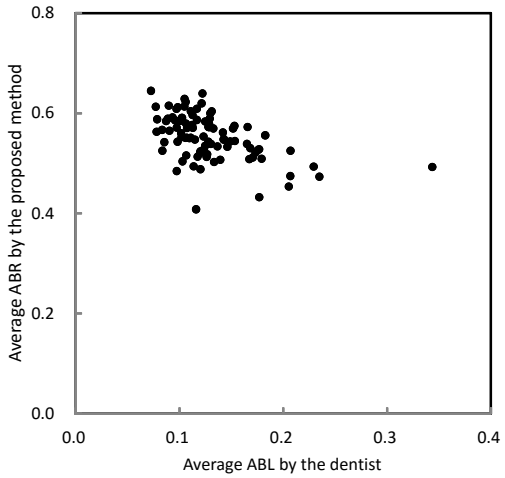

Figure 4. Relationship between average manual ABLs by the dentist and ABRs by the proposed method

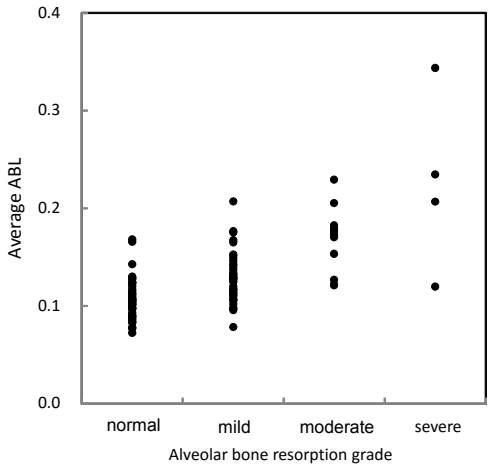

Figure 5. Avrage ABLs for cases with different alveolar bone resorption grades

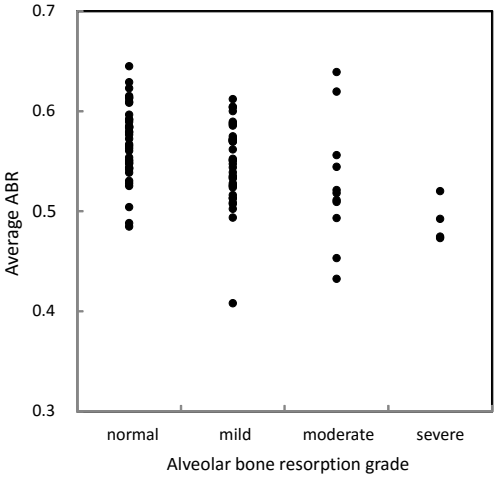

Figure 6. Average ABRs for cases with different alveolar bone resorption grades

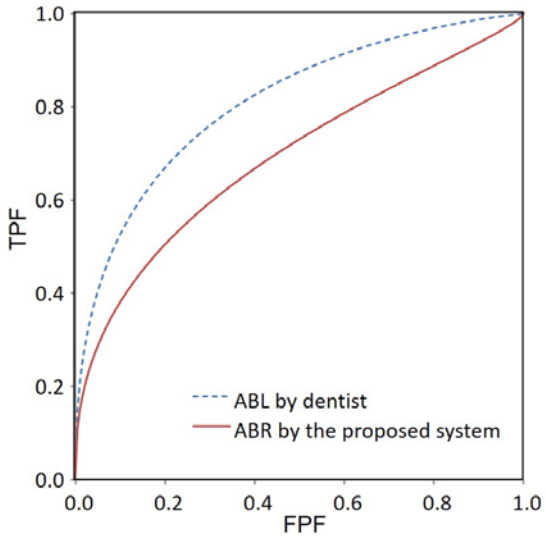

Figure 7. ROC curves for distinction between normal and alveolar resorpion groups by ABL and ABR.

teeth. Other transformation methods with less freedom or a combination of rigid and non-rigid methods should be considered in the future.

V. Conclusion

The experimental result showed moderate correlation between manual ABLs and computerized ABRs determined by the proposed method. The AUC indicates the potential usefulness of the ABRs in detecting patients with alveolar bone resorption. The proposed quantitative method for ABR measurement on DPRs and the image transformation for perceptual assistance may be helpful in efficient diagnosis by dentists. Full automation by detecting tooth crown and root apex points will be studied in the future.

Acknowledgment

Authors appreciate the members of the Fujita Laboratory at Gifu University and dental CAD research group at Asahi University School of Dentistry, Aichi Gakuin University and Media, Co., Ltd. for their valuable discussion.

References

[1] O. Schei, J. Waerhaug, A. Lovdal, A. Arno, “Alveolar bone loss as related to oral hygiene and age,” *J. Periodontol.*, vol. 30, pp. 7-16, Jan. 1959.

[2] M. Zhang, A. Katsumata, C. Muramatsu, T. Hara, H. Suzuki, H. Fujita, “An automatic early stage alveolar-bone-resorption evaluation method on digital dental panoramic radiographs,” in *Proc. SPIE Medical Imaging*, vol. 9035, pp. 90353G-1-90353G-9, 2014.

[3] C. Bishop, *Pattern Recognition and Machine Learning*. New York, NY: Springer Science+Business Media, LLC, 2006, pp. 30.

[4] F. L. Bookstein, "Principal warps: Thin-plate solines and the decomposition of deformations," *IEEE Transactions on Pattern Analysis and Machine Intelligence,* vol. 11, no. 6, pp. 567-585, 1989.